



Supplement of

Intensified future heat extremes linked with increasing ecosystem water limitation

Jasper M. C. Denissen et al.

Correspondence to: Jasper M. C. Denissen (jasper.denissen@bgc-jena.mpg.de)

The copyright of individual parts of the supplement might differ from the article licence.

Sum of models for which $\text{cor}(T_a', ET') > \text{cor}(SW_{in}', ET')$

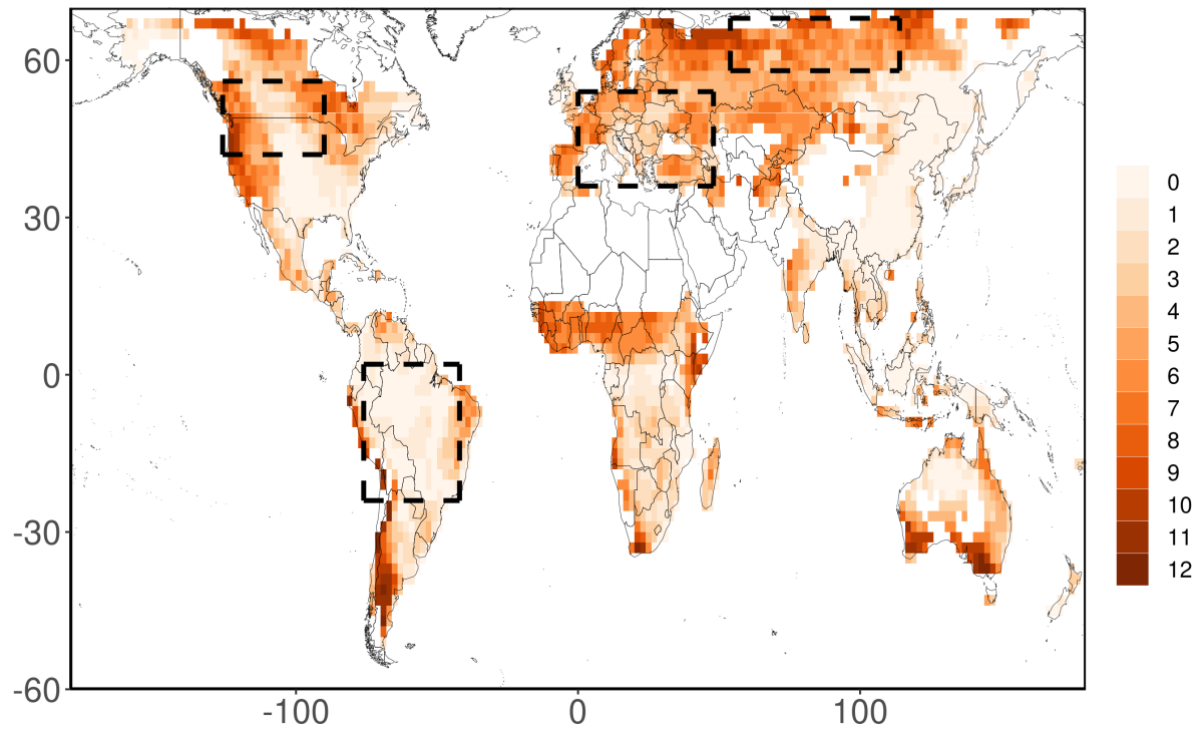


Figure S1: Spatial distribution of the sum of models that are temperature-controlled. Colors show the sum of models for which $\text{cor}(T_a', ET') > \text{cor}(SW_{in}', ET')$ over 1980 – 2100.

Values retained after masking

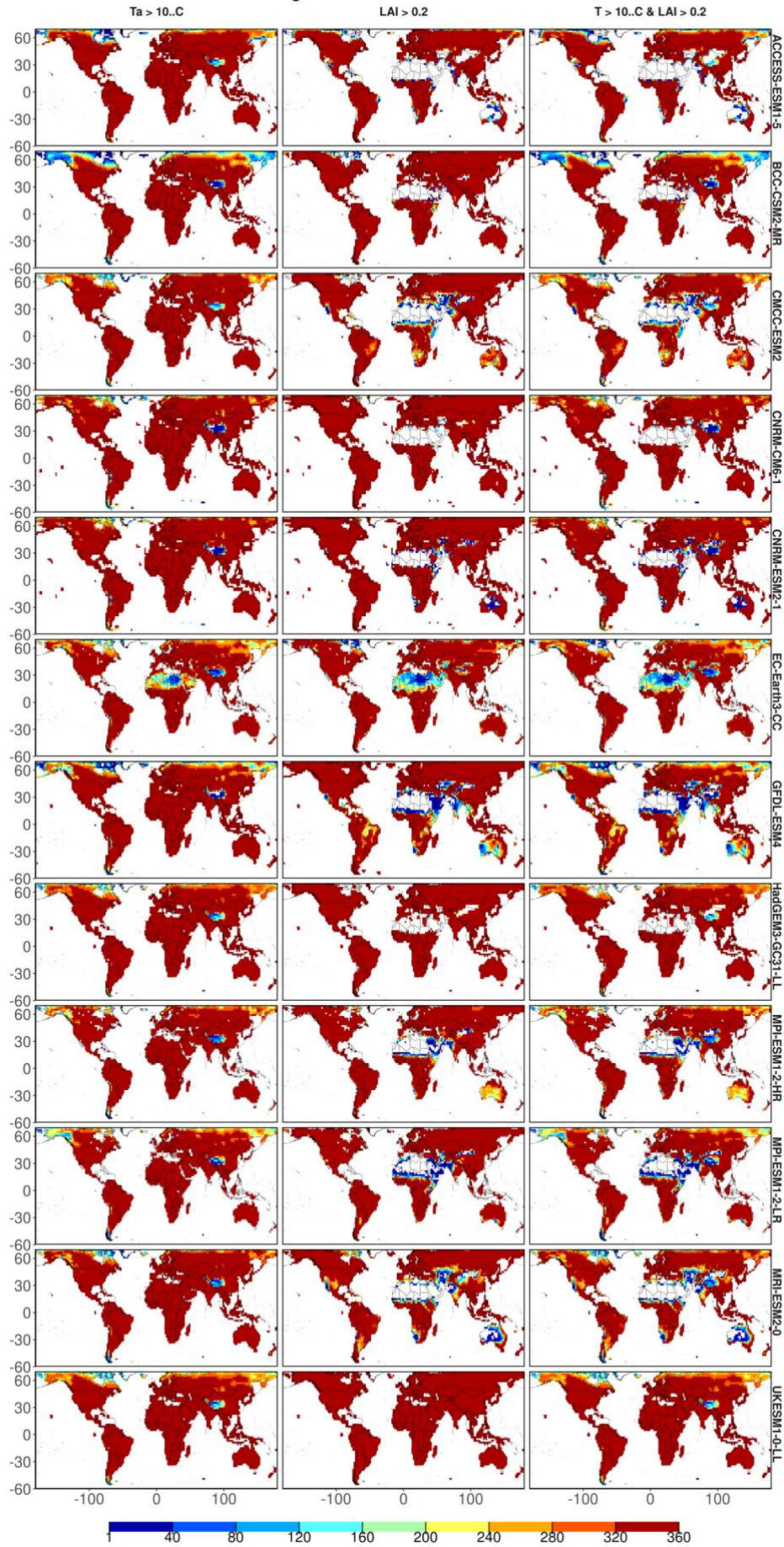


Figure S2: Data points retained after masking. Columns denote the applied filtering procedures (from left to right: $T_a < 10^\circ\text{C}$, $\text{LAI} < 0.5$ and $T_a < 10^\circ\text{C} \ \& \ \text{LAI} < 0.5$). Rows reflect the different individual models. The colors show the amount of values retained after filtering, where the maximum amount of values possible equals 3 hottest months per year over 120 years (360 data points). No data is available in the white regions.

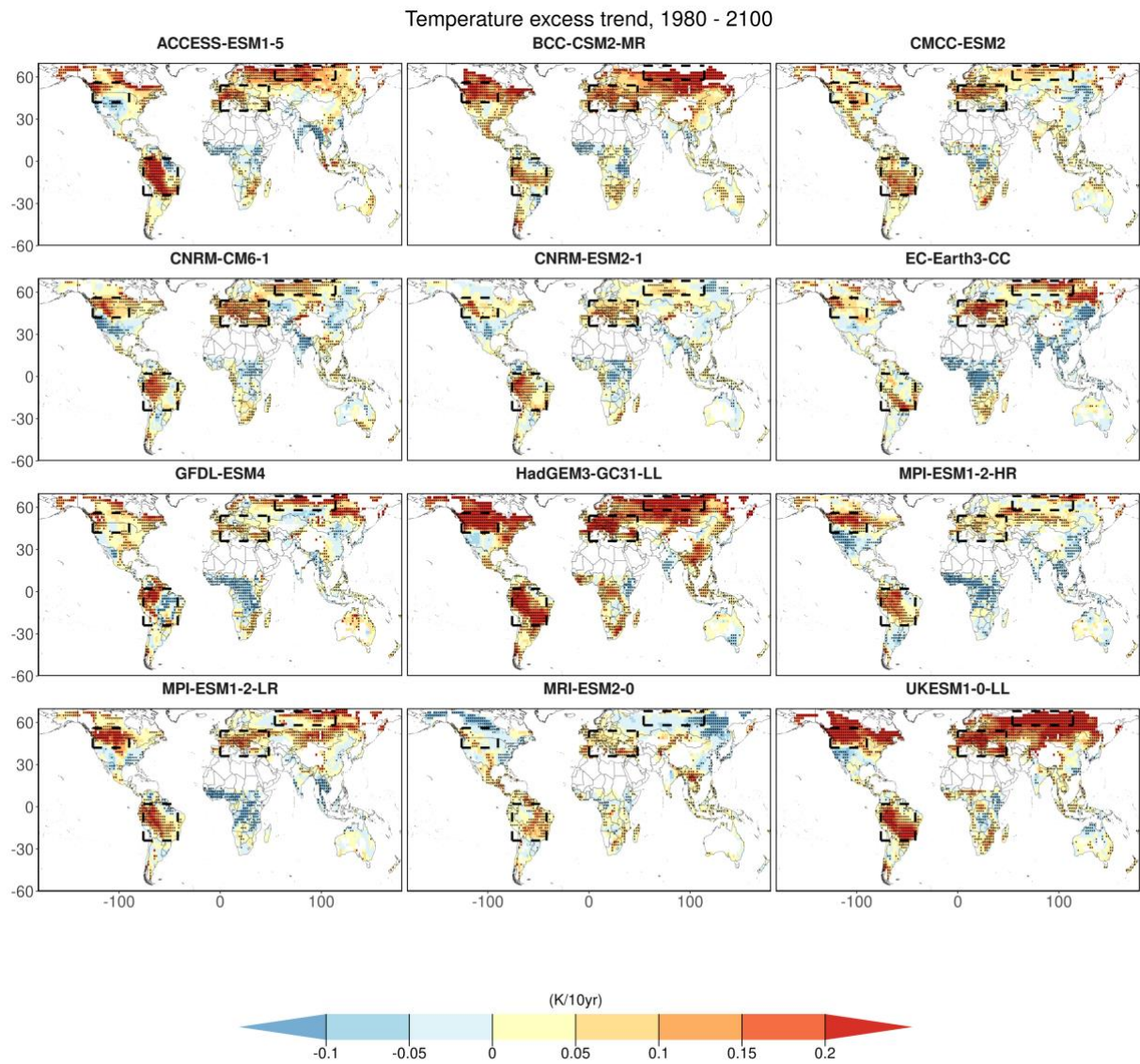


Figure S3: Trends of temperature excess for individual CMIP6 models. The model-specific trends across decadal temperature excess time series (dots indicate significance: $p < 0.05$ based on Kendall's tau statistic).

Incoming shortwave radiation trend, 1980 - 2100

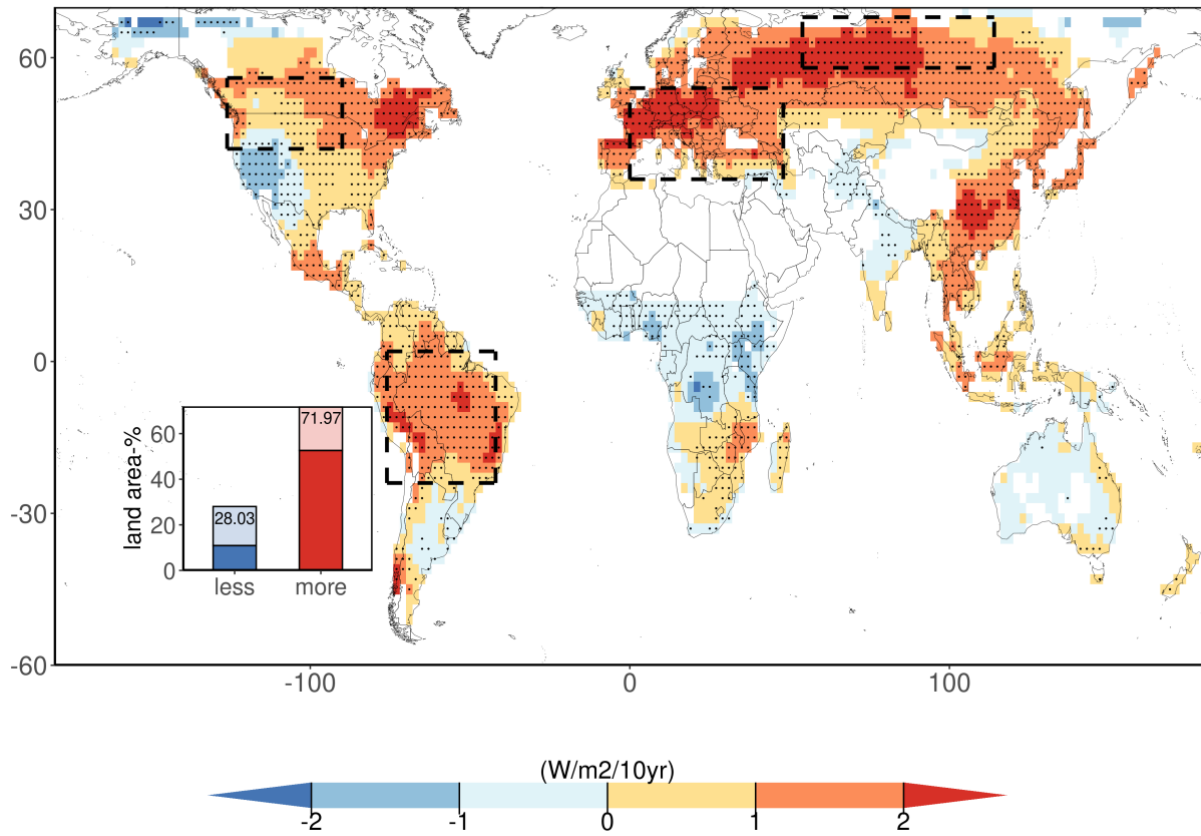


Figure S4: Multi-model mean trend in incoming shortwave radiation based on decadal time series per respective CMIP6 model. The insets display the fraction of the warm land area with positive or negative, respectively (at least 8 out of 12 models agreeing on the sign of the trend are hues darker). Stippling indicates that at least 8 out of 12 CMIP6 models agree on the sign of the trend. All trends are calculated over the warm season and are only displayed if at least 8 CMIP6 models have full time series available, such that white areas denote regions with no or insufficient data. The dashed boxes indicate regions of interest, which are regions where temperature excess increases are particularly rapid and spatially coherent: North and South America (NAM and SAM), Central Europe (CEU) and Northern Asia (NAS) (see Figure 1).

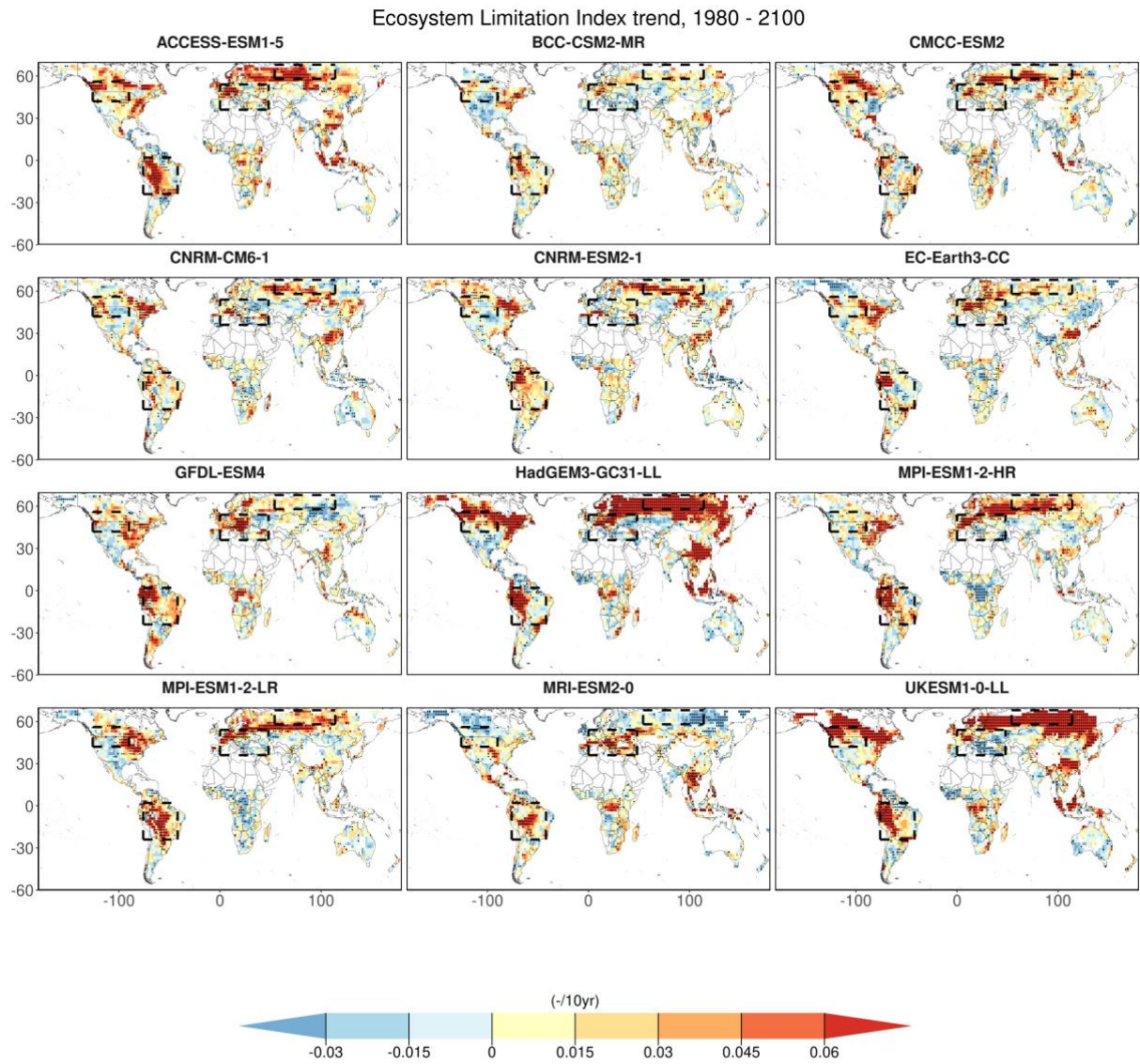


Figure S5: Trends in ecosystem water limitation for individual CMIP6 models. The model-specific trends across decadal ELI time series (dots indicate significance: $p < 0.05$ based on Kendall's tau statistic).

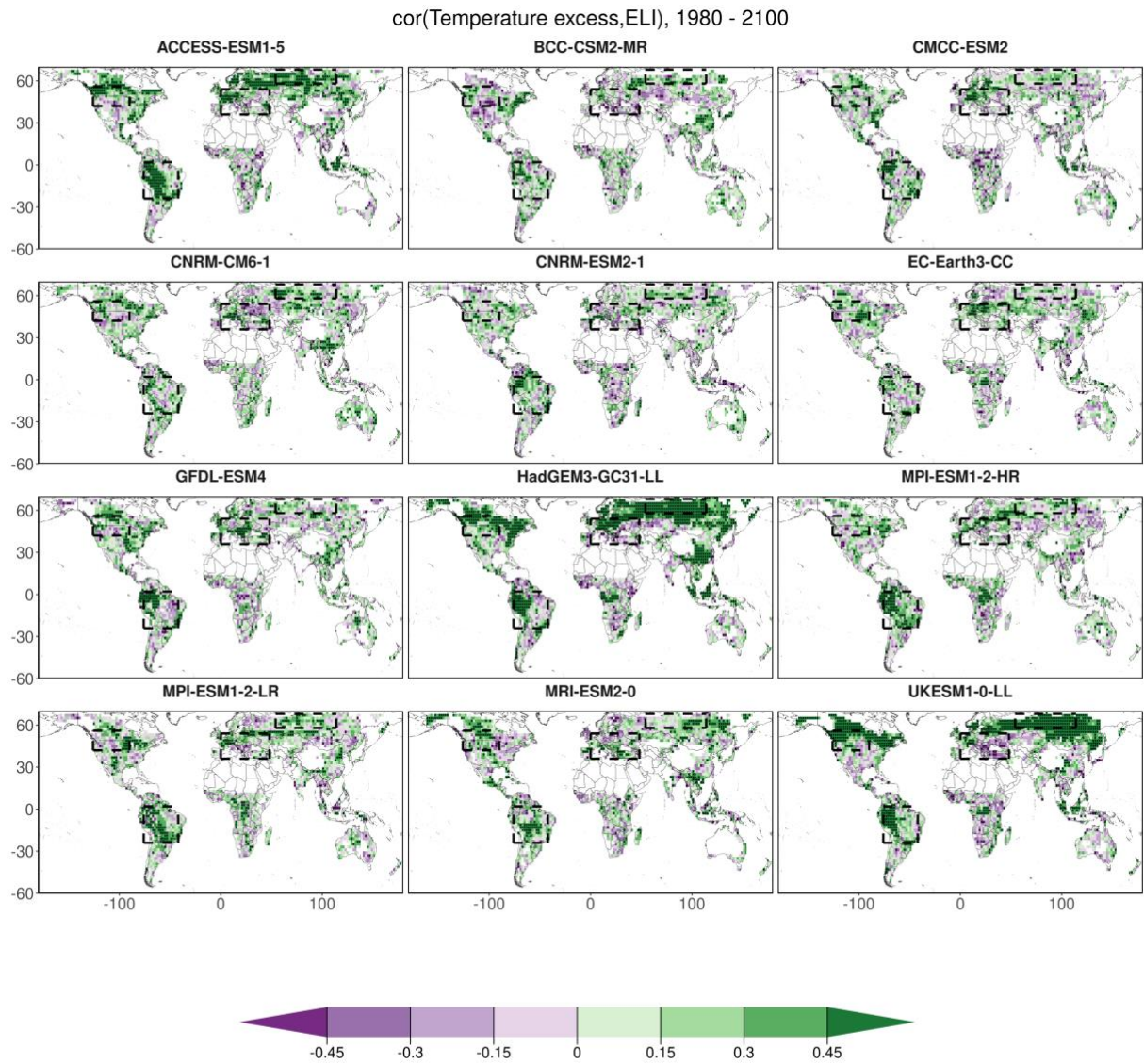


Figure S6: Kendall's rank correlation coefficient between ecosystem water limitation and temperature excess per individual CMIP6 model (dots indicate significance: $p < 0.05$).

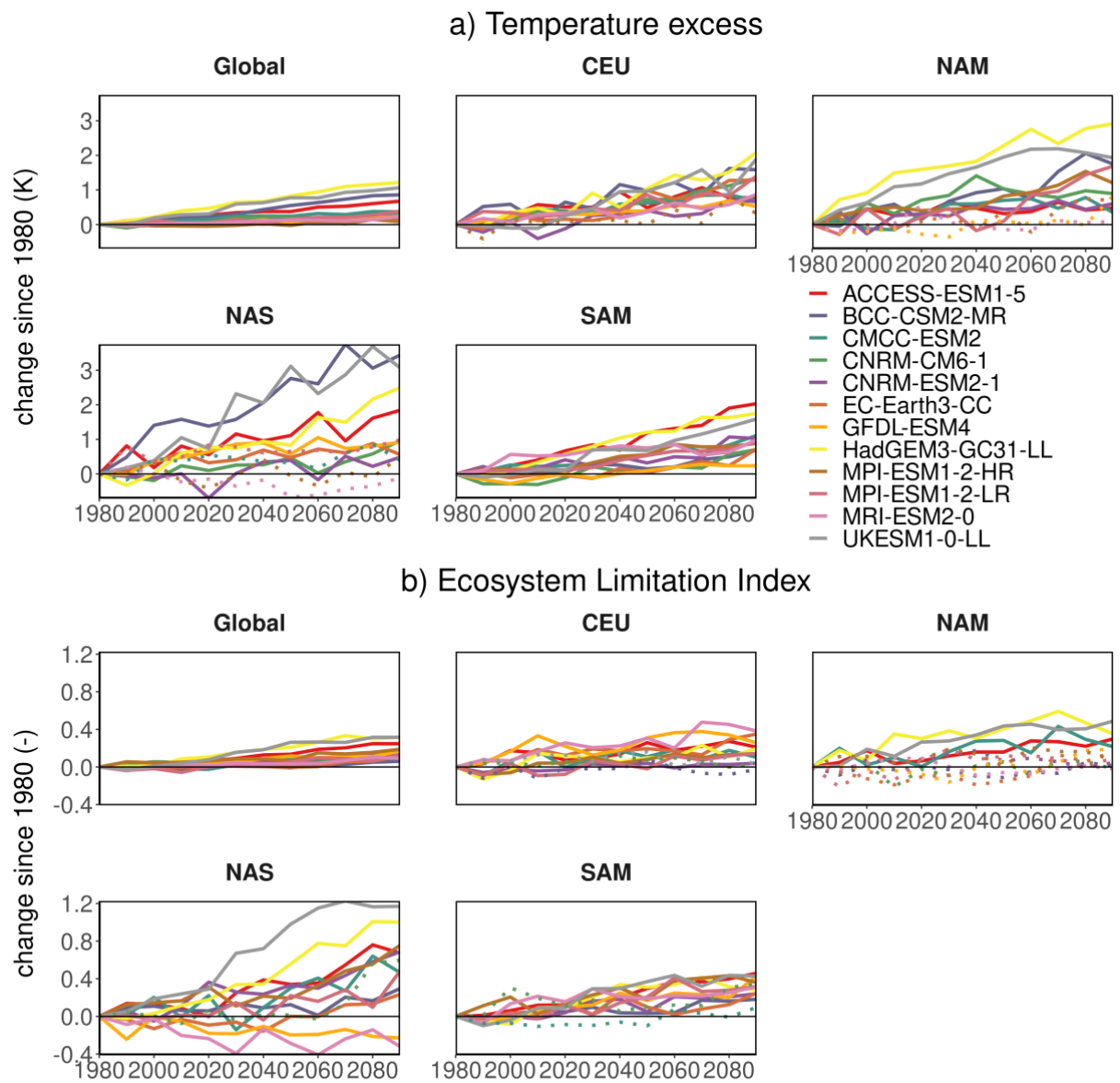


Figure S7: Model-specific changes in global and regional temperature excess in line with increasing ecosystem water limitation. Temporal evolution of a) temperature excess and of b) Ecosystem Limitation Index (ELI) globally and for the regions of interest. Solid lines depict global and regional time series with significant trends ($p < 0.05$ based on Kendall's tau statistic). Global averages are calculated over land grid cells that have complete time series for all models and variables and are weighted according to the surface area per grid cell.

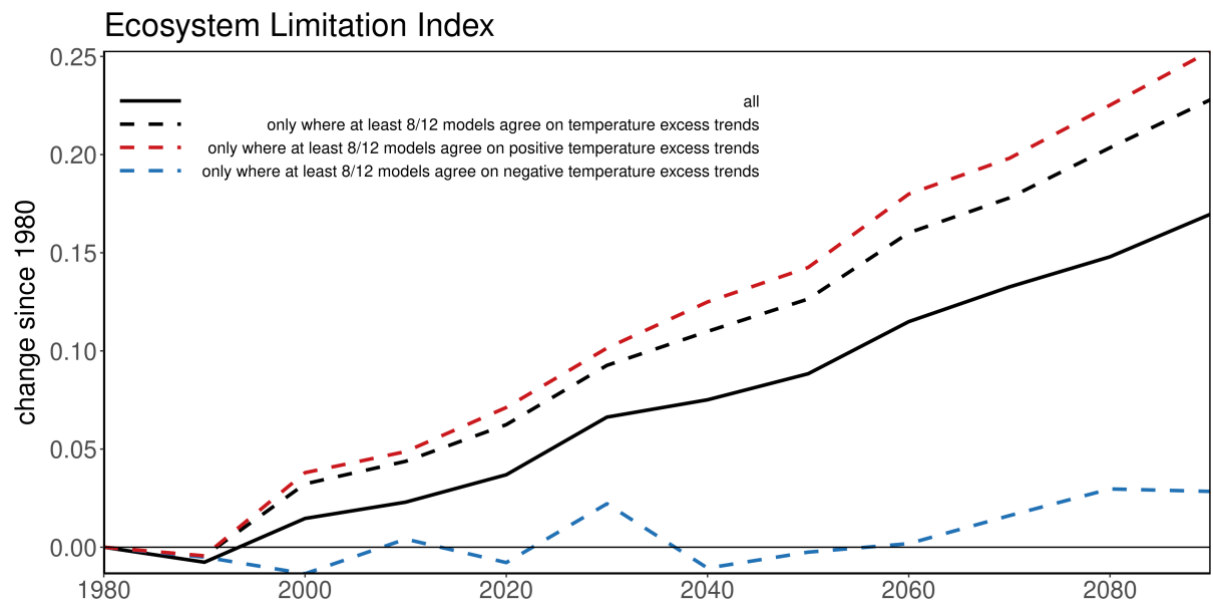


Figure S8: Contrasting trends of ecosystem water limitation from areas with different robustness of temperature excess. All lines depict multi-model mean time series inferred from the model-specific time series. The solid black line is the same as in Figure 2b. The colored dashed lines only consider grid cells where at least 8 out of 12 CMIP6 models agree on temperature excess trends of either sign (black), positive (red) or negative (blue).

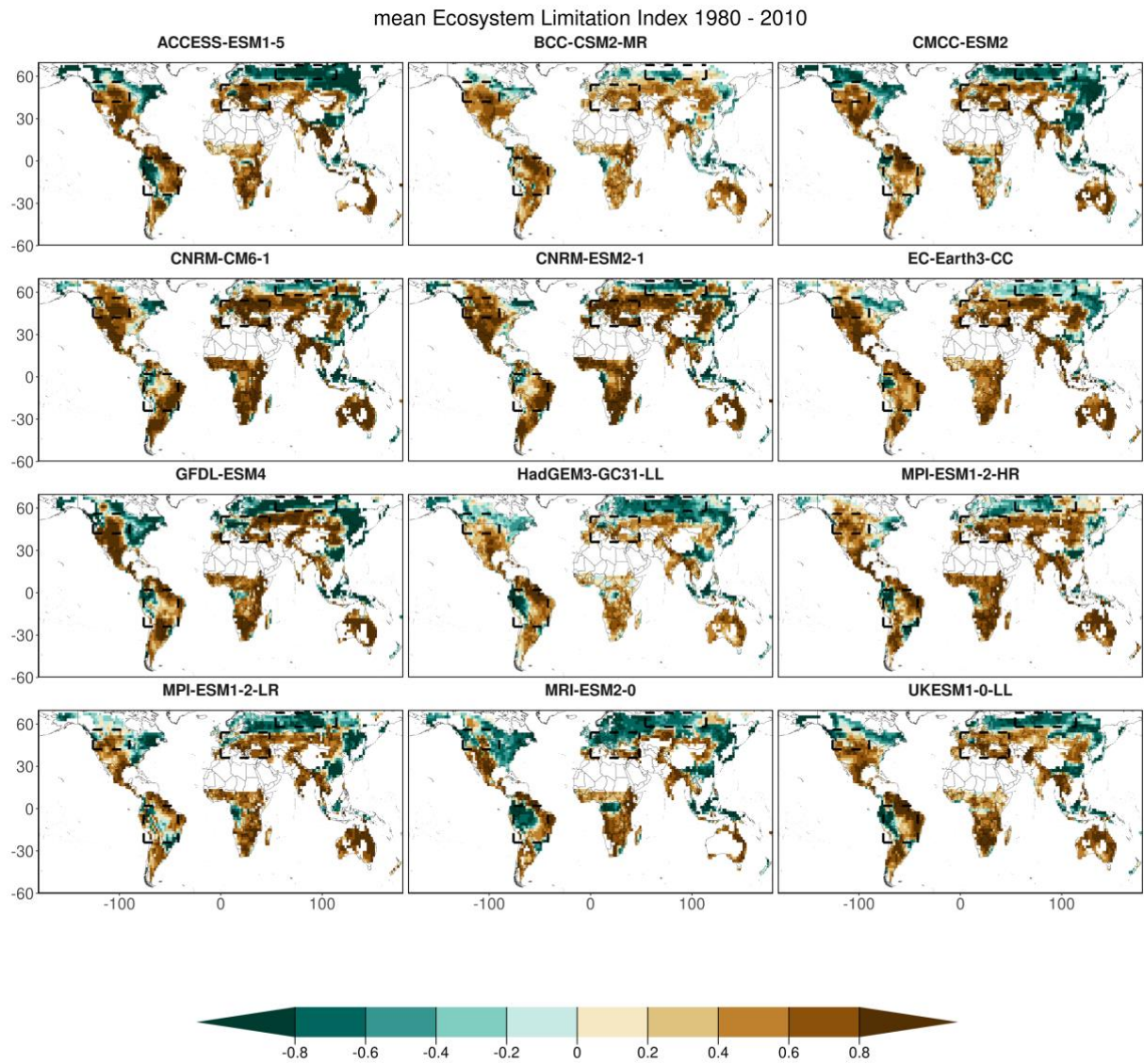


Figure S9: Model-specific initial ecosystem water limitation. Model-specific initial ELI averaged across 1980 - 2010.

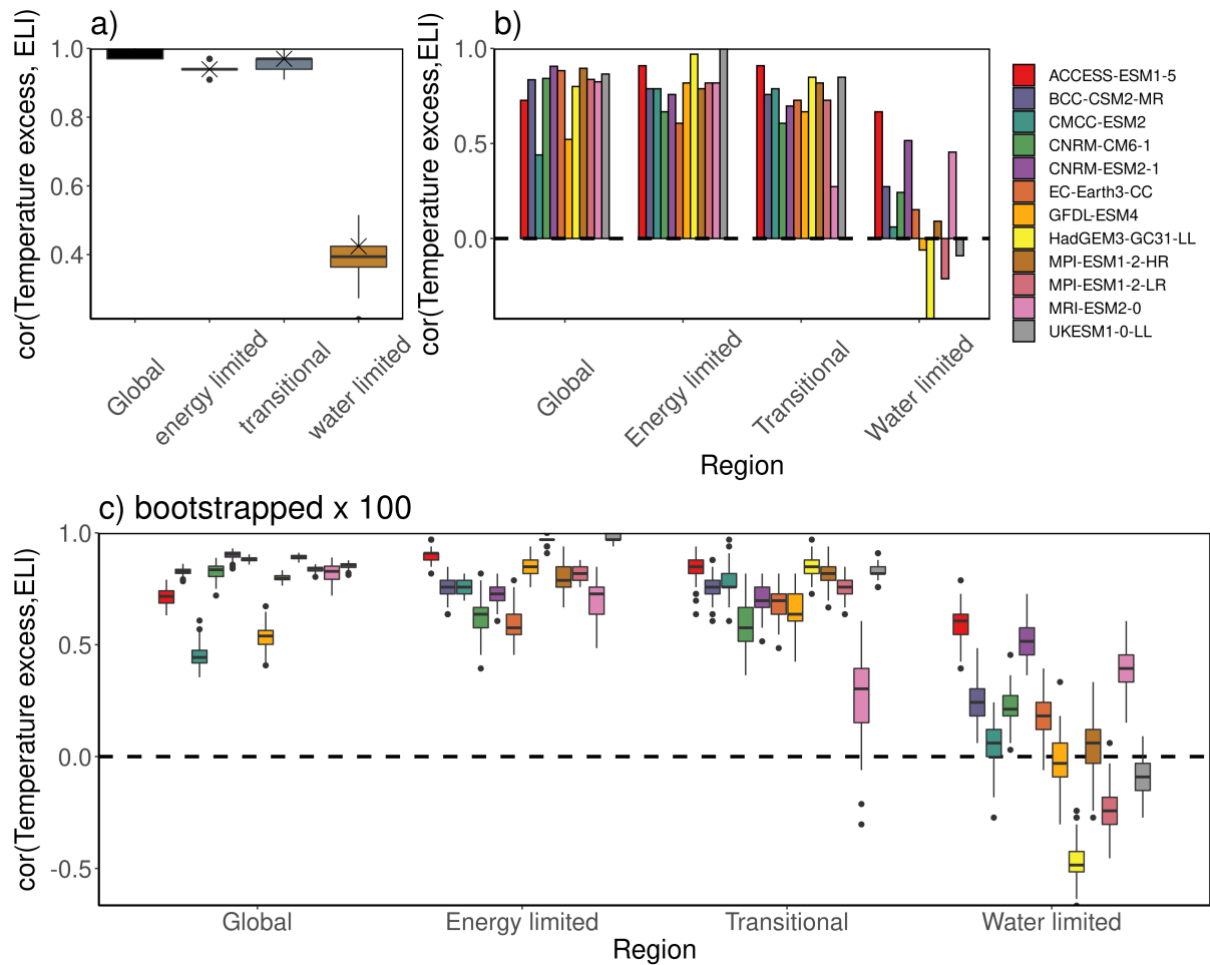


Figure S10: Model-specific global and regional correlations between temperature excess and ecosystem water limitation. a) Correlations between decadal multi-model and regionally averaged time series of temperature excess and ELI, where crosses denote the correlation based on the original data and the box plots denote the uncertainty as obtained from bootstrapping (Methods). b) Barplots of correlations between decadal regionally averaged time series of temperature excess and ELI. c) The same as panel b), but with a hundred estimates obtained from bootstrapping. The regions are defined based on the mean ELI (1980 - 2010; Figure S9): Energy limited ($\text{ELI} < -0.2$), transitional ($-0.2 < \text{ELI} < 0.2$) and water limited ($\text{ELI} > 0.2$).